

Formation and corrosion behavior of Fe-based amorphous metallic coatings prepared by detonation gun spraying

ZHOU Zheng(周 正)^{1,2}, WANG Lu(王 鲁)², WANG Fu-chi(王富耻)², LIU Yan-bo(柳彦博)²

1. College of Materials Science and Engineering, Beijing University of Technology, Beijing 100124, China;

2. School of Materials Science and Engineering, Beijing Institute of Technology, Beijing 100081, China

Received 10 August 2009; accepted 15 September 2009

Abstract: Amorphous metallic coatings with a composition of $\text{Fe}_{48}\text{Cr}_{15}\text{Mo}_{14}\text{C}_{15}\text{B}_6\text{Y}_2$ were prepared by detonation gun spraying process. Microstructural studies show that the coatings present a densely layered structure typical of thermally sprayed deposits with the porosity below 2%. Both crystallization and oxidation occurred obviously during spraying process, so that the amorphous fraction of the coatings decreased to 54% compared with fully amorphous alloy ribbons of the same component. Corrosion behavior of the amorphous coatings was investigated by electrochemical measurement. The results show that the coatings exhibit extremely wide passive region and low passive current density in 3.5% NaCl (mass fraction) and 1 mol/L HCl solutions, which illustrates excellent ability to resist localized corrosion.

Key words: Fe-based amorphous coating; detonation gun; microstructure; corrosion behavior

1 Introduction

During the last few decades, metallic glasses have attained an increasing interest because of their unique physical and chemical properties. However, bulk metallic glasses (BMGs) usually exhibit no plastic deformation after yielding and no work hardening during room temperature deformation due to the formation of highly localized shear bands[1–2], which significantly limits the range of possible applications as engineering and structural materials. To alleviate this case, focusing on their unusual attributes of wear and corrosion resistance, these materials will be more attractive as coatings to withstand aggressive environments[3–4].

Fe-based amorphous metallic glasses are considered to be extremely viable candidates as surface protective coatings owing to their high crystallization temperature, superior corrosion and wear resistance, good magnetic properties, and relatively low material cost[5–7]. Recently, some attempts have been made on preparation of Fe-based amorphous alloy coatings by means of high velocity oxygen fuel(HVOF) and atmospheric plasma spraying(APS) process[8–10]. For example, Fe-Cr-Mo-(C, B, P) coatings exhibited very high amorphous content and excellent corrosion resistance, and Fe-Cr-B-based amorphous coatings expressed extremely

high hardness and prominent erosion resistance. All these researches illustrate the extensively applied prospect of these materials. Nevertheless, the application of detonation gun spraying method, which usually deposits satisfactory coatings with rarely low porosity and high bond strength, to fabricate these materials has been rarely reported. Therefore, in this work, a $\text{Fe}_{48}\text{Cr}_{15}\text{Mo}_{14}\text{C}_{15}\text{B}_6\text{Y}_2$ alloy, with high glass forming ability (GFA) and excellent corrosion resistance[11], was selected to produce amorphous phase coating through detonation spraying method. The microstructural characteristics and corrosion behavior in typical solution of the as-deposited coatings were investigated in detail.

2 Experimental

Powders with nominal composition of $\text{Fe}_{48}\text{Cr}_{15}\text{Mo}_{14}\text{C}_{15}\text{B}_6\text{Y}_2$ (molar fraction, %) were prepared by high pressure argon gas atomization method, then sieved according to conventional sieve analysis and divided into different size ranges. The as-atomized powders with particle size in the range of 40–75 μm were employed for spraying onto ASTM 1045 steel substrates by detonation gun spraying process. All the substrates were degreased by acetone, dried in air, and then grit-blasted prior to deposition. The detailed spraying parameters are presented in Table 1.

Table 1 Detonation spraying parameters utilized in present investigation

Parameter	Processing condition
Oxygen to acetylene volume ratio	1.1
Spraying distance/mm	175
Shot frequency/(cycle·s ⁻¹)	4

The microstructure of the as-deposited coatings was characterized by X-ray diffractometer (XRD), scanning electron microscope (SEM) and transmission electron microscope (TEM). The porosity in the coatings was evaluated by using image analysis on optical microscope (OM). The thermal stability and amorphous fraction of the samples were examined by differential scanning calorimeter (DSC) in a continuous heating mode at a rate of 0.33 K/s under argon atmosphere. Corrosion behavior of the amorphous coatings was investigated by electrochemical measurement on a Potentiostat/Galvanostat (EG&G 273). Electrolytes used were 3.5% NaCl and 1 mol/L HCl aqueous solutions. Electrochemical measurements were conducted in a three-electrode cell using a platinum counter electrode and a saturated calomel reference electrode. The working electrode was exposed only with an area of 1 cm². Potentiodynamic polarization curves were measured with a potential sweep rate of 0.167 mV/s in all the solutions open to air at 298 K after immersing the specimens for 1 h, when the open-circuit potentials became almost steady. For comparison, cast 316L stainless steel plates and 316L stainless steel coatings sprayed by HVOF process were selected to perform the electrochemical measurements in the same way.

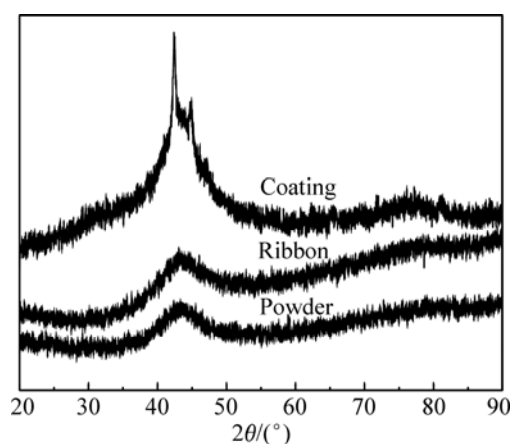
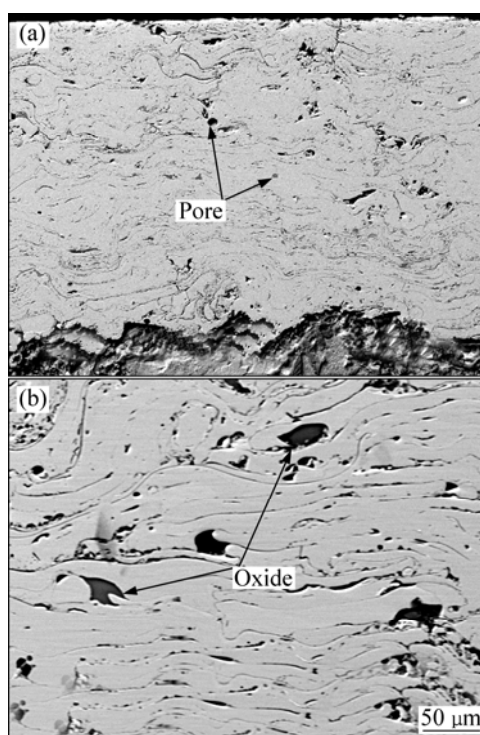
3 Results and discussion

3.1 Microstructure characterization

Fig.1 presents the XRD patterns of the atomized powders, melt-spun ribbon[11] and as-deposited coatings. It is notable that a single broad halo peak appearing in the powder and ribbon samples indicates their high amorphous phase content, which is primarily attributed to the high glass forming ability (GFA) of Fe₄₈Cr₁₅Mo₁₄C₁₅B₆Y₂ alloy system[11], and the origin of this attribute is mainly according to the three empirical rules for the achievement of high GFA[12]. However, the XRD pattern of the coating indicates its partially amorphous phase structure, since the sharp peaks due to crystallization or oxidation are observed obviously on the broad halo peak.

Fig.2 reveals typical regions from cross-sections of the coatings after etching with aqua regia. Generally, the coatings have a dense layered structure, although some pores and microcracks exist as very dark regions can be

seen from the images. The big pores located between flattened droplets are mainly caused by the loosely packed layer structure or gas porosity phenomenon, while the small pores within the flattened particles originate from the shrinkage porosity[13]. In despite of the presence of these defects, the coatings express a low porosity about 1.9% which is typical of detonation sprayed coatings. Furthermore, a fraction of oxides identified as yttrium oxides by energy dispersive spectroscopy (EDS) analysis have been observed occasionally in the coatings, since the yttrium atom has a stronger affinity to the oxygen atom compared with other elements in the alloy system[14]. Oxygen contents in the

**Fig.1** XRD patterns of ribbon, atomized powders and as-deposited coatings**Fig.2** SEM images of cross-sections of as-deposited coatings showing lamellar morphology with some pores (a) and oxides (b)

powders and coatings analyzed using O/N determiner are 0.06% and 2.10% (mass fraction), respectively. Thus, it is concluded that the oxides of the coatings are mainly caused by oxidation during spraying process but not from the original powders.

TEM was undertaken to obtain more detailed information on microstructure formation of the coatings, as shown in Fig.3. The diffused halo ring in the selected area diffraction (SAD) pattern sited on the left bottom of Fig.3 characterizes that the coatings are basically composed of amorphous phase. Nevertheless, also in Fig.3, some nanocrystalline grains can be ascertained to precipitate in the amorphous matrix with grain size in the range of 30–90 nm. It is supposed that the generation of the nanocrystals principally caused by heats accumulated inside the as-deposited coatings. To build up coatings with certain thickness, the spraying gun has to traverse over the previously deposited coatings. This operation leads to the localized reheating both from the direct effect of the gas jet and the latent heat evolutions as successive layers of melted splats solidified. As a result, it could be responsible for the formation of nanocrystalline grains originated from the amorphous matrix.

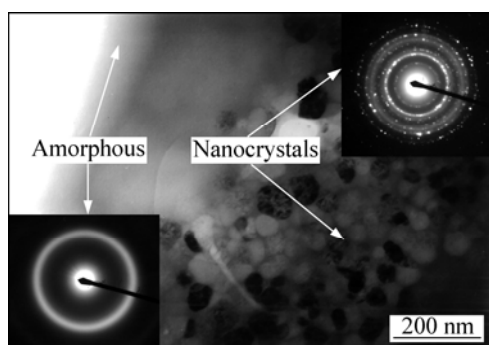


Fig.3 Bright-field TEM images and selected area electron diffraction (SAED) patterns of as-deposited coatings

To clarify the amorphous content of the coatings quantitatively, DSC traces of the coatings, powders and ribbon were examined as well as their heat of crystallization (ΔH), as shown in Fig.4. The volume fraction of amorphous phase in the coatings and powders were calculated by comparison their ΔH value with that of the ribbon standard sample,

$$\eta = \frac{\Delta H_{\text{Coating/Powder}}}{\Delta H_{\text{Ribbon}}} \quad (1)$$

The amorphous fraction (η) of the coatings and powders are about 75% and 54%, respectively, as shown in Table 2, according to the previous conclusions that both crystallization and oxidation occurred during preparation of the coatings. At the same time, the onset crystallization temperature (T_x) of the coatings is

approximately 910 K. That is to say, the coatings with high thermal stability against crystallization can be used in practice reliably and widely.

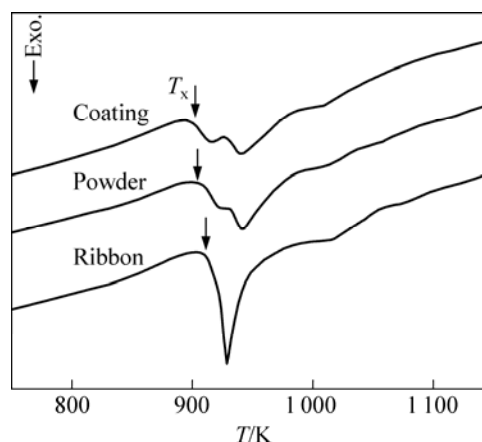


Fig.4 DSC traces of ribbon, atomized powders and as-deposited coatings

Table 2 Thermal analysis results of coating, powder and ribbon

Specimen	T_x /K	ΔH /(J·g ⁻¹)	η /%
Ribbon	920.6	-65.57	100
Powder	916.8	-49.60	75.64
Coating	909.9	-35.44	54.05

3.2 Corrosion behavior

Fig.5 shows the potentiodynamic polarization curves of the Fe-based amorphous coatings deposited by detonation process in comparison with the cast 316L stainless steel plate and HVOF sprayed 316L coating in 3.5% NaCl solution. It is clear that the amorphous coatings exhibit passivated with low passive current density after a short stage of activation, which is attributed to the crystalline phase and oxide distributing diffusely, and also due to structural defects of the coatings including pores and microcracks appearing

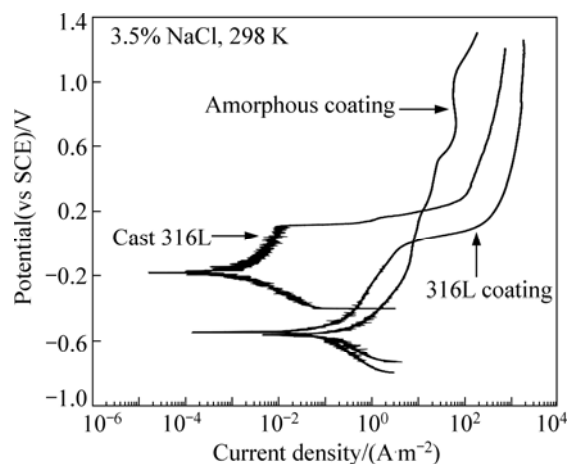


Fig.5 Potentiodynamic polarization curves of amorphous coating, in comparison with cast 316L stainless steel plate and 316L coating in 3.5% NaCl solution open to air at 298 K

occasionally. The tiny fluctuation of the passive region implies alternant process of active solution and passivation for the same reason mentioned above. However, the transpassive potential of the amorphous coating is as high as 1.0 V associating with an extremely wide passive region, which suggests that amorphous coatings have a prominent ability to resist localized corrosion. In contrast, the comparatively limited passive regions of both 316L plate and coating indicate a low ability to withstand localized corrosion, such as pitting. Therefore, Fe-based amorphous coatings fabricated by detonation spraying could be effective as surface protective films in marine environments.

The corrosion behavior of the amorphous coatings in 1 mol/L HCl solution, as shown in Fig.6, is similar to their performance in 3.5% NaCl solution. Nevertheless, the values of their passive current density are a little higher than those in NaCl solution, which illustrates a weakened ability for the surface passive films to keep stable. However, wide passive regions are recognized with similarly high transpassive potential, 0.9 V, as those observed in NaCl solution. That is to say, the amorphous coatings basically retain the superior corrosion properties to resist localized corrosion in 1 mol/L HCl solution. Unfortunately, the corrosion resistance of both 316L stainless steel plate and coating declines rapidly in 1 mol/L HCl solution compared with their performance in 3.5% NaCl solution. The 316L plate displays a high passive current density combined with a very narrow passive region, and the 316L coating even undergoes active dissolution at a low potential without any distinct passivation. Therefore, the corrosion resistance of the amorphous coatings in the corrosive environments containing chloride ions to induce pitting, such as NaCl and HCl solutions, is further superior to 316L stainless steel materials.

The high resistance to pitting corrosion of the

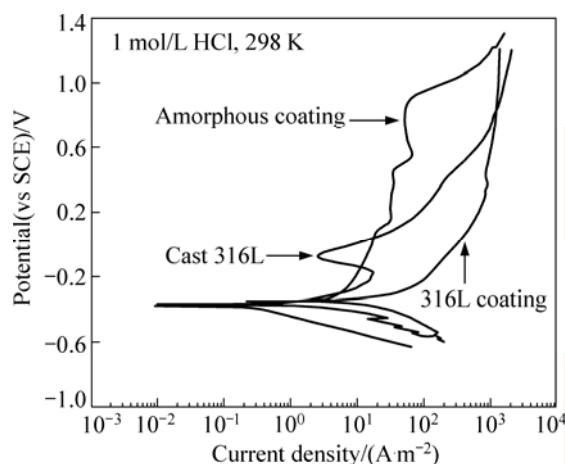


Fig.6 Potentiodynamic polarization curves of amorphous coatings in comparison with cast 316L stainless steel plate and 316L coating in 1 mol/L HCl solution open to air at 298 K

amorphous alloys is considered to be primarily determined by the characteristic of forming a homogeneous phase structure without grain boundaries which are sensitive to chloride ions absorption[15]. Moreover, chromium-rich passive surface films formed on Fe-Cr-based metallic glasses prevent the evolution of corrosion[6], and molybdenum improves further the corrosion resistance and passivating ability[16], since it prevents dissolution of chromium during passivation. Furthermore, the high amorphous phase content of the coatings here provides the formation of a uniform passive film and hence also contributes to their high corrosion resistance.

4 Conclusions

1) $\text{Fe}_{48}\text{Cr}_{15}\text{Mo}_{14}\text{C}_{15}\text{B}_6\text{Y}_2$ amorphous metallic coatings were prepared by detonation gun spraying process with the porosity below 2%.

2) The amorphous fraction of the as-deposited coatings is approximately 54%, although some nanocrystals and yttrium oxide come out during spraying process. And the onset crystallization temperature of the coatings approaches 910 K.

3) The amorphous coatings exhibit excellent ability to resist localized corrosion in 3.5% NaCl and 1 mol/L HCl solutions, which is further superior to 316L stainless steel.

References

- [1] LOUZGUINE D V, KATO H, INOUE A. High-strength Cu-based crystal-glassy composite with enhanced ductility [J]. *Applied Physics Letters*, 2004, 84(7): 1088–1089.
- [2] INOUE A. Stabilization of metallic supercooled liquid and bulk amorphous alloys [J]. *Acta Materialia*, 2000, 48(1): 279–306.
- [3] GREER A L, RUTHERFORD K L, HUTCHINGS I M. Wear resistance of amorphous alloys and related materials [J]. *International Materials Reviews*, 2002, 47(2): 87–112.
- [4] ZANDER D, KOSTER U. Corrosion of amorphous and nanocrystalline Zr-based alloys [J]. *Mater Sci Eng A*, 2004, 375/377(1/2): 53–59.
- [5] SHEN B L, INOUE A, CHANG C T. Superhigh strength and good soft-magnetic properties of (Fe,Co)-B-Si-Nb bulk glassy alloys with high glass-forming ability [J]. *Applied Physics Letters*, 2004, 85(21): 4911–4913.
- [6] PANG S J, ZHANG T, ASAMI K. Bulk glassy Fe-Cr-Mo-C-B alloys with high corrosion resistance [J]. *Corrosion Science*, 2002, 44(8): 1847–1856.
- [7] INOUE A, MAKINO A, MIZUSHIMA T. Ferromagnetic bulk glassy alloys [J]. *Journal of Magnetism and Magnetic Materials*, 2000, 215: 246–252.
- [8] OTSUBO F, KISHITAKE K. Corrosion resistance of Fe-16%Cr-30%Mo-(C, B, P) amorphous coatings sprayed by HVOF and APS processes [J]. *Materials Transactions*, 2005, 46(1): 80–83.
- [9] CHOKETHAWAI K, MCCARTNEY D G, SHIPWAY P H. Microstructure evolution and thermal stability of an Fe-based amorphous alloy powder and thermally sprayed coatings [J]. *Journal of Alloys and Compounds*, 2009, 480(2): 351–359.
- [10] WU Y P, LIN P H, CHU C L, WANG Z H, CAO M. Cavitation erosion characteristics of a Fe-Cr-Si-B-Mn coating fabricated by high

- velocity oxy-fuel (HVOF) thermal spray [J]. *Materials Letters*, 2007, 61(8/9): 1867–1872.
- [11] ZHOU Zheng, WANG Lu, WANG Fu-chi, ZHANG Hai-feng, CHENG Huan-wu, LIU Yan-bo, XU Sai-hua. Effects of yttrium on the glass-forming ability and corrosion resistance of Fe_{50-x}Mo₁₄Cr₁₅C₁₅B₆Y_x amorphous alloys [J]. *Transaction of Beijing Institute of Technology*, 2008, 28(5): 455–463. (in Chinese)
- [12] INOUE A. High strength bulk amorphous alloys with low critical cooling rates [J]. *Materials Transactions, JIM*, 1995, 36(7): 866–875.
- [13] SOBOLEV V V, GUILMANY J M. Investigation of coating porosity formation during high velocity oxy-fuel (HVOF) spraying [J]. *Materials Letters*, 1994, 18(5/6): 304–308.
- [14] DO H K, JIN M P, JOON S P, JONG H N, DONG H K. Effect of Y addition on thermal stability and the glass forming ability in Fe-Nb-B-Si bulk glassy alloy [J]. *Mater Sci Eng A*, 2006, 435/436: 425–428.
- [15] PANG S J, ZHANG T, ASAMI K, INOUE A. Synthesis of Fe-Cr-Mo-C-B-P bulk metallic glasses with high corrosion resistance [J]. *Acta Materialia*, 2002, 50(3): 489–497.
- [16] KAWAKITA J, KURODA S, FUKUSHIMA T, KODAMA T. Improvement of corrosion resistance of oxyfuel-sprayed stainless steel coatings by addition of molybdenum [J]. *Journal of Thermal Spray Technology*, 2005, 14(2): 224–230.

(Edited by YANG Hua)